Biomed Microdevices (2013) 15:657–663
DOI 10.1007/s10544-013-9788-2

Electrical field manipulation of cancer cell behavior monitored by whole cell biosensing device

Evangelia Hondroulis · Steven J. Melnick · Xueji Zhang · Ze-Zhi Wu · Chen-Zhong Li

Published online: 23 June 2013

Abstract All living cells possess electrical characteristics and are thus responsive to, and even generate electric fields and currents. It has been shown that the electrical properties of cancer cells differ from normal proliferating cells, thus electric fields may induce differential effects in normal and cancer cells. Manipulation of these electrical properties may provide a powerful direct and/or adjuvant therapeutic option for cancer. A whole cell impedance-based biosensor to monitor the effects of a range of different frequencies (50 kHz–2 MHz) at low-intensity (<2 V/cm) on the growth rate of human SKOV3 ovarian cancer cells versus non-cancerous HUVECs is reported. Rapid real-time monitoring of the SKOV3 behavior was observed as the alternating electric fields were applied and the impedimetric response of the cells was recorded. The cells were also labeled with propidium iodide to examine morphological changes and cell viability with fluorescence microscopy with trypan blue for comparison. A noticeable decrease in the growth profile of the SKOV3 was observed with the application of 200 kHz alternating electric fields indicating specific inhibitory effects on dividing cells in culture in contrast to the HUVECs. The outcome of this research will improve our fundamental understanding of the behavior of cancer cells when exposed to alternating electric fields at specific frequencies and foster the development strategies and optimal parameters for alternating electric field therapies for clinical and drug delivery applications.

Keywords Electrotherapy · Cancer · Cell electronics · Intermediate frequency field · Biosensor · Impedance

E. Hondroulis · C.-Z. Li (✉)
Nanobioengineering/Bioelectronics Laboratory, Department of Biomedical Engineering, Florida International University, 10555 West Flagler Street, Miami, FL 33174, USA
e-mail: licz@fiu.edu

S. J. Melnick
Department of Pathology and Clinical Laboratories, Miami Children's Hospital, Miami, FL, USA

X. Zhang
Research Center for Bioengineering and Sensing Technology, University of Science and Technology Beijing, Beijing 100083, China

Z.-Z. Wu
Key Laboratory of Biorheological Science and Technology of the State Ministry of Education, College of Bioengineering, Chongqing University, Chongqing 400044, People's Republic of China

1 Introduction

Electrically directed and coordinated cell movement plays a significant role in mammalian cell behavior starting from embryonic development. The effects of exogenous electric fields on physiology and their possible relationship to diseases have interested researchers for years (Barker et al. 1984; Ieran et al. 1990; Sandyk 1997). The use of electric fields has become popular in fields such as gene and cellular therapies (Golzio et al. 2002; Song et al. 2004; Teissié et al. 2008), and has even progressed to clinical trials for drug delivery (Fantozzi et al. 2010), however; still little is known how electric fields may interact with intracellular signaling pathways to potentially alter cell physiology.

Living cells are associated with electrical characteristics due to the cell membrane transport processes and are thus responsive to and even generate electric fields and currents. Cells control the exchange of electrically charged ions across their membrane creating a membrane potential with different amounts of electrical charges inside and outside the cell. A shift in membrane potential will alter the exchange of ions across it and vice versa. For instance, it has been shown that alteration in membrane potential can alter the signal pathways involved in mitosis of the cell and thus its proliferation (Blackiston et al. 2009).

Recently, there has been interest in the therapeutic use of alternating electric fields as a treatment for cancer. Since the electrical and physical properties of cancer cells differ from normal proliferating cells, electric fields may induce differential effects in normal and cancer cells. For example, cancer cells exhibit a lower membrane electrical potential compared to normal cells. Cancer cells also exhibit disorganized growth, weak interactions with their neighboring cells and do not exhibit contact inhibition of their growth (Lock et al. 2010). Consequently further research is warranted to establish the role of electric field therapy for the treatment of cancer.

Biosensors are valuable tools for monitoring cell behavior because they can provide information about the total physiological responses of cells to external stimuli. Most current biosensors are used to detect enzymes, DNA/RNA and immunological components (Luong et al. 2008). Biosensors that measure cellular properties in whole cells may have an advantage over other biosensors because they can provide information about various properties of cells in the viable state. This study will use a whole cell-based array-formatted electrical impedance sensing system (EIS) (Hondroulis et al. 2010, 2012) to monitor the effects of external alternating electric fields on the behavior of ovarian cancer cells HTB-77™ (SKOV3) compared to normal human umbilical vascular endothelial cells CRL-1730™ (HUVEC). The electric fields tested are within a range of frequencies (50 kHz–2 MHz) and at low-intensity (<2 V/cm). Electric fields with these properties have been shown to inhibit growth *in vivo* (Kirson et al. 2007) in support of this line of research. The biosensor employed will measure in real-time the electrode surface impedance changes produced by growing cell monolayers over the electrodes and detecting any changes in resistance associated with changes in the cell layer after electric field exposure. The benefits of using this biosensor compared to the *in vivo* study are the shortening of the experimental procedure as multiple experimental conditions can be performed with the array setup, and the capability of visually monitoring the behavior of the cells under the electric fields in real time. A range of electric field parameters will be used to determine the greatest degree of growth inhibition for these types of cancer cell lines.

2 Materials and methods

2.1 Cell culture

HTB-77™ and CRL-1730™ cells were purchased from American Type Culture Collection (ATCC, Rockville, MD, USA) and were cultured in McCoy's 5A Modified Medium and Dulbecco's Modified Eagle Medium respectively, each containing 10 % fetal bovine serum, 0.3 mg ml^{-1} L-glutamine, 100 U ml^{-1} penicillin and 100 mg ml^{-1} streptomycin. The cell cultures were placed in an incubator (37 °C, 5 % CO_2 atmosphere) for 24 h prior to the experiment so that the cells reached confluency with a final concentration of 10^5 cells ml^{-1}. 0.4 ml of cell suspension was inoculated into each well in the EIS chip for the experiments.

2.2 Electrical impedance sensing (EIS)

The EIS chip design was previously reported (Hondroulis et al. 2010). In short, individual tissue culture wells of volume $9\times9\times10$ mm^3 are placed over an array of eight detecting gold electrodes (250 μm in diameter) each linked to a gold counter electrode (7×46 mm^2) (Fig. 1). The impedance of the circuit with a resistance and a capacitor in series can be measured for each well by applying an alternating current (approximately 1 μA) to the electrodes present in the EIS chip through a 1 MΩ resistor. As cells are placed in each well, they settle down onto the electrode surface creating a barrier for the flowing current increasing the impedance and resistance measurements. From Ohm's law, V = I R, it is possible to monitor the cell attachment and proliferation from the increase in impedance or resistance measurements.

2.3 Application of external electric field

To incorporate the external electric field to the EIS chip, a unique system of a pair of insulated wires (BLK KYNAR 100′, conductor area 0.25 mm) was designed to be placed in conjunction with the 8 well array design of the EIS chip. The wires were placed in 4 of the wells with the other 4 wells used as the control. The wires were placed 1 mm apart to allow spacing to encompass the whole electrode area. Figure 2 shows a schematic of the wire setup and the resulting electric field surrounding the electrodes. A Leader LFG-1300S Function Generator was used to provide the square AC waves at the desired frequencies.

2.4 Immunofluorescence staining

Propidium iodide (PI) was purchased from Calbiochem (San Diego, CA) and diluted to 50 μg/ml with DI water. 10^5 cells/ml were added to standard petri dishes, one with wires placed on the bottom spaced 1 mm apart to apply an external electric field of 200 kHz and one without wires as the control. 25 μl of PI was added to each dish and incubated in the dark for 10 min. Fluorescence intensity was determined using a confocal microscope (Perkin Elmer UltraView Vox system, USA). With an excitation wave length of 530 nm and an emission filter of 620 nm. PI attaches to the DNA of the cell, and thus cells with broken membranes will be targeted.

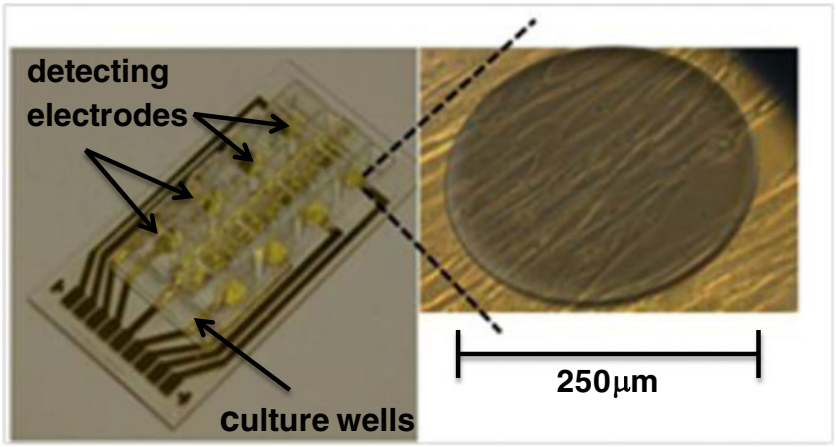

Fig. 1 Design of the electrical impedance sensing chip showing the array of eight detecting gold electrodes. The cells attach on the electrode surface altering the measured resistance values

2.5 Cell viability assay

Trypan blue was purchased from Sigma Aldrich. 10^5 cells/ml were added to standard petri dishes, one with wires placed on the bottom spaced 1 mm apart to apply an external electric field of 200 kHz and one without wires as the control. After 40 h, the cells were removed with 0.25 % trypsin/EDTA (GIBCO), alloquotted into centrifuge tubes and were spun for 5 min at 100 × g. The supernatant was discarded and the cells were resuspended with 1 ml PBS (Fisher Scientific). A 1:1 ratio of 0.4 % Trypan Blue and cell suspension was made and was allowed to sit for 3 min for the cells to incorporate the dye. 20 μl of the cell suspension was then added to a hemocytometer to perform a cell count. The % viability was calculated using the following equation:

$$\text{viable cells}(\%) = \frac{\text{total number of viable cells per ml of aliquot}}{\text{total number of cells per ml of aliquot}} \times 100$$

3 Results

3.1 Optimal frequency

Five frequencies of alternating electric fields that sample a broad radiofrequency range, 50, 100, 150 and 200 kHz and 2 MHz, were tested on both SKOV3 and HUVEC to find the optimal frequency that would most hinder the growth of the SKOV3 cells without harming the normal HUVECs. Intermediate frequencies of around 100 kHz have previously been reported to not have any detrimental effects on cells (Elson 1995), however, according to Kirson et al. (2007), specific types of cancer cells may behave differently under the range of 100 kHz to 300 kHz frequencies with the theory that the electric fields disrupt the normal mitotic process of proliferating cells. The choice of frequencies is in part based on this study. Frequencies in the lower (50 kHz) and higher (2 MHz) range were also included.

Using the EIS biosensor, we monitored the proliferation rate of the cells under the influence of the alternating electric fields in real-time by analyzing the change in resistance values of the detecting electrodes. Proliferating cells will gradually attach and spread across the electrode surface creating an increase in resistance values. Any change in

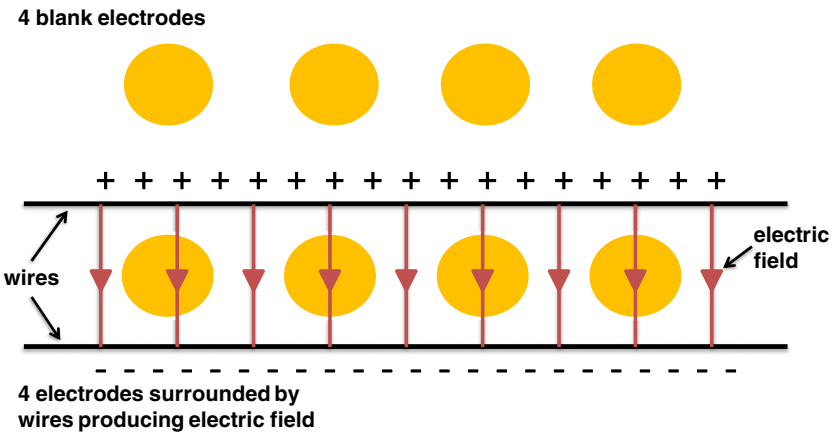

Fig. 2 Schematic of wire setup for application of external alternating electric fields to the EIS chip. The two wires (*black lines*) were spaced at approximately 1 mm apart to encompass the entire electrode (*gold circles*) on the EIS chip. The *red lines* represent the resulting electric field generated with the *arrows* pointing in the direction of the field

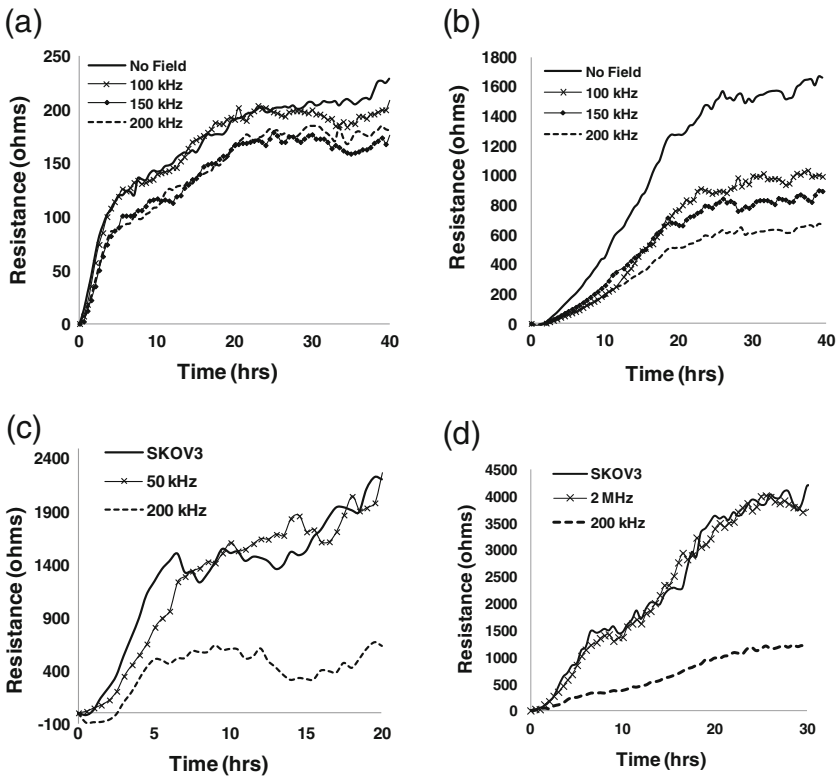

Fig. 3 Resistance values of HUVECs (**a**) and SKOV3 (**b**) under electric fields of frequencies 100, 150 and 200 kHz. No apparent effect was noticed for the normal HUVECs, however, a significant decrease in resistance values was observed for the SKOV3 for all three frequencies. For further comparison, 50 kHz (**c**) and 2 MHz (**d**) frequencies were tested on SKOV3 and showed no apparent effect on the cell proliferation as seen in the similar resistance curves to the control. 200 kHz showed the largest decrease out of all the frequencies

proliferation is detected by a decrease the resistance values. Figure 3a and b show the resistance values obtained from the HUVECs and the SKOV3 respectively in the target range under 100, 150 and 200 kHz applied at the start of the run compared to the cells alone, both over a timeframe of 40 h.

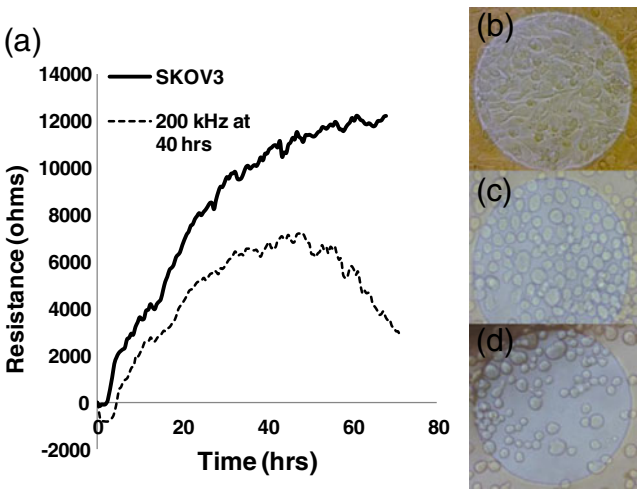

Fig. 4 Resistance values of SKOV3 cells when subjected to 200 kHz electric field after 40 h on the electrode (**a**). Digital images were taken of this electrode to visualize the cell attachment process. Figure 4b shows the electrode after the cells reached confluency over the electrode. After this, the 200 kHz field was applied and within an hour another image was taken (**c**). The cells have changed morphology to a more rounded shape compared to the initial image. After an additional 40 h of exposure to the electric field, another image was taken (**d**) which shows a significant decrease in cell number on the electrode

The EIS biosensor was able to detect no noticeable difference in the resistance values when the alternating electric field was applied to the HUVECs compared to the control, thus indicating no obvious effect of the electric fields of the three frequencies on the HUVECs proliferation.

In contrast, the SKOV3 had lower resistance values compared to the control with 200 kHz providing the lowest resistance values out of the three frequencies. These results indicate that the growth and proliferation rate of the SKOV3 was hindered by the alternating electric field at each frequency evaluated with 200 kHz being the most effective frequency. The resistance values still increased over time with the applied external electric fields; however, the overall values were lower than the control. This difference can be attributed to a slower rate of proliferation and attachment of the cells to the electrodes and thus showing growth inhibition. For justification that this range of frequencies is optimal for disrupting the SKOV3 cell proliferation, 50 kHz and 2 MHz frequencies were tested as well on the SKOV3 and were compared with the results from 200 kHz (Fig. 3c, d respectively). Neither 50 kHz nor 2 MHz affected the SKOV3 proliferation compared to the 200 kHz frequency, and thus we focused more closely on this frequency.

3.2 Focus on 200 kHz

In the subsequent experiment, the 200 kHz field was applied to the cells after they reached confluency on the EIS electrodes.

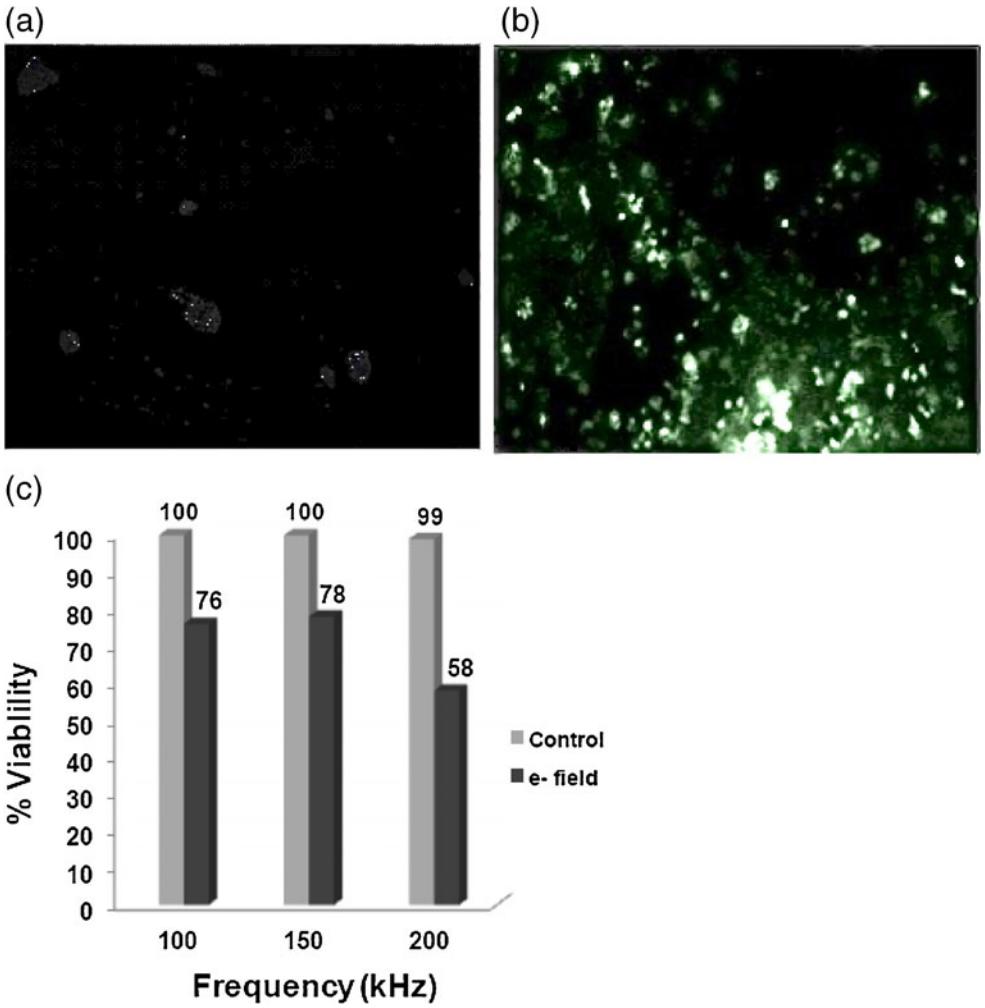

Fig. 5 Fluorescence imaging using propiduim iodide (PI). SKOV3 cells were grown on petri dish, one control (**a**) with no external electric field and one with wires providing 200 kHz frequency (**b**). After 40 h, the cells were stained with PI and the cells exposed to 200 kHz showed significant cell death as seen in the increase in fluorescence compared to the control. To further justify the effects of the 200 kHz electric field on SKOV3, Trypan Blue exclusion test for cell viability was performed for 100, 150 and 200 kHz (**c**). 200 kHz showed the lowest percent viability of 58 %

This was done to determine whether the field affected the cells before or after attachment. Most cell types need to attach to a substrate in order to proliferate, however, it has been shown that cancer cells have a lower tendency for adhesion which in turn could lead to metastasis (Hirohashi 1998). The SKOV3 were placed in the wells with the wires in place at the beginning of the run without applying the external electric field. The resistance changes produced by the attachment of cells to the electrodes were monitored for 40 h, allowing the cells to reach confluency, and then the 200 kHz field was applied. With the addition of the field, there was a noticeable decrease in resistance values over time indicating disruption of cell attachment to the electrodes (Fig. 4a).

In addition to the measurement of resistance, the effects of the alternating electric fields on the SKOV3 cells were evaluated by examining digital images taken of one of the detecting electrodes; the electrode with SKOV3 cells after 40 h once they reached confluency the electrode after 1 h of 200 kHz applied field to the confluent cells and the electrode after another 40 h of exposure to the electric field (Fig. 4b, c, d respectively). Prior to the application of the alternating electric field, the image of the electrode shows a confluent monolayer of cells covering it as is expected without any external stimulus. Normal proliferating cells attached to a substrate will have a flattened morphology as they extend themselves along the surface as shown in Fig. 4b. However, once the 200 kHz electric field was applied, the cell morphology changed to a more round shape even after only an hour of exposure to the field, indicating a disruption in the attachment of the cells to the electrode. Finally, after 40 h of exposure to the electric field, the cell number diminished significantly indicating a disruption in the cell proliferation.

3.3 Immunofluorecence staining and cell viability assay

Two additional methods for measuring cell viability after exposure to the alternating electric fields were performed to independently correlate the results obtained by the EIS. Immunofluorecence images were taken using PI, a fluorescent molecule that binds to the DNA of cells. Since PI is impermeable to cell membranes, viable cells will not incorporate the molecule and thus it can be used for cell viability assays. Figure 5a and b show the fluorescence images of the SKOV3 without and with the 200 kHz field after 40 h of

exposure respectively. The cells that were subjected to the field showed more fluorescence than the control indicating a higher occurrence of cell death.

Trypan Blue exclusion test for cell viability was also performed. Trypan Blue is a dye that cannot penetrate the intact cell membranes of viable cells, thus indicating the total amount of viable cell in a sample. Figure 5c is a chart showing the percent viability estimated by the number of attached SKOV3 after exposure to the alternating electric fields in the target range of 100, 150 and 200 kHz. Similar to the EIS data, after exposure to 200 kHz, the cells exhibited the least amount of cell viability.

4 Discussion

Research on the effects of alternating electric fields on biological samples has been a growing interest for biomedical researchers over the years. Cells have intrinsic electrical properties that are implicit to metabolism and other cellular functions. Many of the electrical properties are derived from the cellular membrane consisting of a lipid bilayer embedded with various transmembrane proteins creating ionic channels that comprise the cell's transmembrane potential. Evidence suggests that cellular properties such as proliferation, adhesion, differentiation, morphology and migration, and function are influenced by external alternation electric fields suggesting a relationship between these properties and the electrical properties of cells. A deeper understanding of this relationship will yield a more comprehensive view of cell function and the role that electric field therapies may play in the treatment of diseases such as cancer.

Cancer cells have been shown to have different membrane properties than regular cells. One property that may play a large role in cancer behavior is the membrane fluidity since cancer cells seem to have higher membrane fluidity than non-cancer cells. Increased membrane fluidity also affect the cell's motility and deformation (Sok et al. 2002) leading to a hindered cell–matrix adhesion and ultimately specific cell responses that influence cell adhesion, motility, shape, orientation, differentiation, and survival. Cells that are attached and thus capable of proliferating have a flattened appearance due to cell spreading. As we have shown, once subjected to the field, the SKOV3 cells changed morphology within only an hour of exposure to the 200 kHz applied field. The cells acquired a more round shape which could be attributed to the increase in membrane fluidity of the cells under the electric field.

Another important feature for cell survival is the membrane potential. Cancer cells also exhibit an increase in negative surface charge of their membrane (Szachowicz-Petelska et al. 2010) compared to normal cells and thus have cell membrane potentials that are lower than the cell membrane potential of healthy cells. When subjected to external electric fields, the membrane experiences most of the potential drop in the cell leading to conformational changes in proteins and enzymes embedded within the membrane ultimately affecting the cell's capability for proliferation and differentiation (Tsong 1990). For example, biochemical and physiological changes occur when weak electric currents are applied to a cell due to a change in transmembrane potential induced on the cell membrane. Since the membrane is flexible, permeation of the cell membrane occurs leading to a higher exchange of materials across the membrane, a process known as electroporation (Mir 2001). This process has been widely used in biomedical research in areas such as drug delivery (Charoo et al. 2010; Zhao et al. 2010) and gene transfer (Lin and Dean 2011) because of its reversibility. In this study, we show that a low intensity electric field at 200 kHz has a detrimental effect on cancerous SKOV3 cells without affecting the non cancerous HUVEC cells.

5 Conclusion

Many current treatments for cancer are effective; however, a major limitation in these treatments is their toxicities and side effects. Electric field therapies as an adjuvant for cancer treatment show considerable promise; however, further preclinical and clinical investigation is required. The outcome of this research will improve our fundamental understanding of the behavior of cancer cells to alternating electric fields and define a strategy and optimal parameters of electrotherapy for clinical and drug delivery applications. This whole cell-based biosensor will enhance our understanding of the responsiveness of cancer cells to electric field therapy and demonstrate potential therapeutic opportunities for electric field therapy in the treatment of cancer.

Acknowledgments This research and development project was supported by the grant NIH R15 ES021079-01, Young Inventor Award by W. H. Coulter Foundation to Cz Li, and the Research Foundation for Doctoral Programs in Universities under the State Ministry of Education of China (No. 20100191110032) to Zz Wu.

References

A.T. Barker, R.A. Dixon, W.J.W. Sharrard, M.L. Sutcliffe, Lancet **323**, 994–996 (1984)

D.J. Blackiston, K.A. McLaughlin, M. Levin, Cell Cycle **8**, 3527–3536 (2009)

N.A. Charoo, Z. Rahman, M.A. Repka, S.N. Murthy, Curr. Drug Deliv. **7**, 125–136 (2010)

E. Elson, in *The biomedical engineering handbook*, ed. by J.D. Bronzino (CRC Press, Inc, Boca Raton, 1995), pp. 1417–1423

F. Fantozzi, E. Arturoni, R. Barbucci, Bioelectrochemistry **78**, 191–195 (2010)

M. Golzio, J. Teissié, M.P. Rols, PNAS **99**, 1292–1297 (2002)
S. Hirohashi, Am. J. Pathol. **153**, 333–339 (1998)
E. Hondroulis, C. Liu, C.Z. Li, Nanotechnology **21**, 315103 (2010)
E. Hondroulis, Z. Zhang, C. Chen, C.-Z. Li, Anal. Lett. **45**, 272–282 (2012)
M. Ieran, M. Bagnacani, M. Annovi, A. Moratti, R. Cadessi, J. Orthop. Res. **8**, 276–282 (1990)
E.D. Kirson, V. Dbaly, F. Tovarys, J. Vymazal, J.F. Soustiel, A. Itzhaki, D. Mordechovich, S. Steinberg-Shapira, Z. Gurvich, R. Schneiderman, Y. Wasserman, M. Salzberg, B. Ryffel, D. Goldsher, E. Dekel, Y. Palti, PNAS **104**, 10152–10157 (2007)
X. Lin, D. Dean, Am. J. Respir. Crit. Care Med. **183**, A2099 (2011)
F.E. Lock, N. Underhill-Day, T. Dunwell, D. Matallanas, W. Cooper, L. Hesson, A. Recino, A. Ward, T. Pavlova, E. Zabarovsky, M.M. Grant, E.R. Maher, A.D. Chalmers, W. Kolch, F. Latif, Oncogene **29**, 4307–4316 (2010)
J.H.T. Luong, K.B. Male, J.D. Glennon, Biotechnol. Adv. **26**, 492–500 (2008)
L.M. Mir, Bioelectrochemistry **53**, 1–10 (2001)
R. Sandyk, J. Altern. Complement. Med. **3**, 365–386 (1997)
M. Sok, M. Sentjurc, M. Schara, J. Stare, T. Rott, Ann. Thorac. Surg. **73**, 1567–1571 (2002)
L. Song, L. Chau, Y. Sakamoto, J. Nakashima, M. Koide, R. Tuan, Mol. Ther. **9**, 607–616 (2004)
B. Szachowicz-Petelska, I. Dobrzynska, S. Sulkowski, Z.A. Figaszewski, J. Environ. Biol. **31**, 845–850 (2010)
J. Teissié, J. Escoffre, M. Rols, M. Golzio, Radiol. Oncol. **42**, 196–206 (2008)
T.Y. Tsong, Annu. Rev. Biophys. Biophys. Chem. **19**, 83–106 (1990)
X. Zhao, M. Zhang, R. Yang, Commun. Nonlinear Sci. Numer. Simul. **15**, 1400–1407 (2010)